The reliability of age measurements for Young Stellar Objects from Hertzsprung-Russell or color-magnitude diagrams

Research in Astron. Astrophys. **2012** Vol. **12** No. **1**, 1–25
http://www.raa-journal.org *http://www.iop.org/journals/raa*

Research in Astronomy and Astrophysics

INVITED REVIEWS

The reliability of age measurements for Young Stellar Objects from Hertzsprung-Russell or color-magnitude diagrams

Thomas Preibisch

Universitäts-Sternwarte München, Ludwig-Maximilians-Universität, Scheinerstr. 1, 81679 München, Germany; *preibisch@usm.uni-muenchen.de*

Received 2011 September 30; accepted 2011 October 4

Abstract The possibility to estimate ages and masses of Young Stellar Objects (YSOs) from their location in the Hertzsprung-Russell diagram (HRD) or a color-magnitude diagram provides a very important tool for the investigation of fundamental questions related to the processes of star formation and early stellar evolution. Age estimates are essential for studies of the temporal evolution of circumstellar material around YSOs and the conditions for planet formation. The characterization of the age distribution of the YSOs in a star forming region allows researchers to reconstruct the star formation history and provides important information on the fundamental question of whether star formation is a slow or a fast process. However, the reliability of these age measurements and the ability to detect possible age spreads in the stellar population of star forming regions are fundamentally limited by several factors. The variability of YSOs, unresolved binary components, and uncertainties in the calibrations of the stellar parameters cause uncertainties in the derived luminosities that are usually much larger than the typical photometry errors. Furthermore, the pre-main sequence evolution track of a YSO depends to some degree on the initial conditions and the details of its individual accretion history. I discuss how these observational and model uncertainties affect the derived isochronal ages, and demonstrate how neglecting or underestimating these uncertainties can easily lead to severe misinterpretations, gross overestimates of the age spread, and ill-based conclusions about the star formation history. These effects are illustrated by means of Monte-Carlo simulations of observed star clusters with realistic observational uncertainties. The most important points are as follows. First, the observed scatter in the HRD must not be confused with a genuine age spread, but is always just an upper limit to the true age spread. Second, histograms of isochronal ages naturally show a decreasing number of stars for ages above the median, a pattern that can be misinterpreted as an accelerating star formation rate. Third, it is emphasized that many star forming regions consist of several sub-groups, which often have different ages. If these distinct stellar populations cannot be disentangled (e.g., due to projection effects) and the HRD of all stars in the region is used for an age analysis, it is very difficult (often impossible) to discern between the scenario of an extended period of star formation (i.e. a large age spread) and the alternative concept of a temporal sequence of several discrete star formation episodes. Considering these factors, most observations of star forming regions suggest that age spreads are usually smaller than the corresponding crossing times, supporting the scenario of fast and dynamic star formation.

Key words: stars: ages — stars: pre–main sequence — stars: formation — Hertzsprung-Russell diagram

1 INTRODUCTION

Since stars are the fundamental building blocks of our universe, the process of star formation is of central importance in astrophysics. This process starts with the collapse of a molecular cloud core that quickly forms a central protostar surrounded by a large reservoir of circumstellar material in the form of a dense envelope. Due to the requirement of angular momentum conservation, the infalling matter in the envelope cannot fall directly on the central protostar, but rather forms a torus or disk-like structure perpendicular to the rotation axis. These circumstellar disks are a fundamental characteristic of a Young Stellar Object (YSO, hereafter). The physical processes in the circumstellar disk and its evolution govern the final outcome of the star formation process. Some fraction of the circumstellar matter is accreted onto the protostar, some part is ejected as a protostellar jet and outflow, and a large fraction is dispersed, mainly by photoevaporative flows driven by the radiation from the central protostar.

The circumstellar disks are the sites where planets are born; they are thus often denoted as "proto-planetary" disks. How exactly the dust and gas in the disk are transformed into a planetary system is one of the most interesting current areas of star formation research. As more and more extrasolar planetary systems are discovered, detailed studies of the proto-planetary disks in YSOs are required to provide information about the initial conditions in which these planets have formed. General descriptions of the evolution of YSOs and the planet formation process can be found in the monographs of Hartmann (2001a), Stahler & Palla (2005), Armitage (2010), Ward-Thompson & Whitworth (2011) and Garcia (2011), the proceedings of the *Protostars and Planets V* conference (Reipurth et al. 2007), as well as the recent reviews of Williams & Cieza (2011) and Armitage (2011).

As discussed in the next section, reliable information on the ages of YSOs is of central importance for many aspects of the star and planet formation process. This paper is focused on the uncertainties in the determination of stellar ages (and masses) and the identification of possible age spreads in star forming regions and young clusters. The most widely used approach to estimate ages of young stars is quite simple: one just has to establish the effective temperature and the luminosity of a young star from the observational data and place it into a Hertzsprung-Russell diagram (HRD); the age and mass of the star can then be found by comparison with theoretical pre-main sequence (PMS) evolutionary models. The dispersion of the age values derived for a sample of stars contains information about the age spread in the population. In contrast to the apparent simplicity of this procedure, the interpretation of the resulting isochronal age values and their dispersion is not straightforward but requires a careful consideration of the observational uncertainties and a number of effects that can considerably adulterate the derived ages. While most of these effects are rather small (or even absent) in stellar populations that are at least a few tens of mega-years (Myr) old, they can substantially affect the derived stellar parameters if YSOs with circumstellar material are considered. The purpose of this paper is to demonstrate how neglecting or underestimating these uncertainties can easily lead to biased or even wrong conclusions.

The structure of this paper is as follows: In Section 2, I discuss the importance of age estimates for young stars. Section 3 provides a brief description of the basic properties of YSOs and discusses the important issue of variability in YSOs. In Section 4, I describe the effect of the observational uncertainties on the ages derived from an HRD and illustrate this by means of Monte-Carlo simulations. Section 5 is devoted to the problems that arise if only photometric but no spectroscopic data are available and ages are inferred from a CMD. In Section 6, I discuss further factors that can mimic age spreads in actual co-eval populations. Section 7 briefly comments on the reliability of stellar parameters derived from fits to the broad-band spectral energy distributions. Finally, Section 8 summarizes the conclusions from these considerations.

2 THE IMPORTANCE OF AGE MEASUREMENTS FOR YSOS

The mass and the age are the two most important parameters of a star. The stellar mass determines the evolution path and the final fate of the star, while the stellar age tells us in which stage of its evolution the star is. Unfortunately, both parameters usually can not be directly measured, but have to be inferred from measurements of other stellar parameters, such as the luminosity and effective temperature, via comparison to theoretical stellar evolution models. Stellar masses can sometimes be determined with high precision by observations of the motions in binary systems; this provides an important calibration and quality check for the theoretical stellar models. Stellar ages, on the other hand, are generally more difficult to determine (see Soderblom 2010, for a comprehensive overview). However, reliable age determinations are of fundamental importance for our understanding of the star formation process as well as the temporal evolution of YSOs and their circumstellar material.

Reliable information on stellar ages is required for any study of the temporal evolution of the circumstellar material around YSOs. Recent results suggest that protoplanetary disks evolve very quickly and are dispersed within quite short timescales of just a few Myr. Already at an age of 5 Myr, a large majority ($\geq 80\%$) of all YSOs has lost at least their inner disks (see Briceño et al. 2007). These short disk lifetimes put very strong constraints on the theories of planet formation, in particular for the formation of Jupiter-like gas giants.

Measurements of the age dispersion in the stellar population of a star forming region provide information about a possible age spread and can allow researchers to reconstruct the star formation history; this provides crucial tests for different star formation theories. The star formation process is closely related to the properties and evolution of the interstellar medium in and out of which the stars form. Our understanding of interstellar clouds has experienced a considerable paradigm change during the last decade. Early models were based on quasi-static equilibrium models of clouds that were thought to be in virial equilibrium and evolve on long time scales (i.e. many crossing times) of order $\gtrsim 10^8$ yr (e.g., Solomon et al. 1979). Accordingly, star formation was considered to be a slow process, and the stellar populations in star forming regions should thus exhibit a large spread of individual stellar ages. However, new observations suggest that the interstellar medium is highly dynamic and strongly affected by supersonic turbulence (see Ballesteros-Paredes et al. 2007). This is impressively illustrated by recent results from the *Herschel* space observatory that show that most clouds do not resemble quasi-static roughly spherical entities, but have a very elongated, filamentary structure (e.g., André et al. 2010; Molinari et al. 2010). Most current models of the interstellar medium suggest that the evolution of the clouds is dominated by the action of supersonic turbulence and large-scale flows; the turbulence generates the filamentary structures and creates density enhancements that become gravitationally unstable and form stars (e.g., Ballesteros-Paredes & Hartmann 2007; Elmegreen 2007; Heitsch et al. 2008; Hennebelle et al. 2008; Banerjee et al. 2009). According to these ideas, molecular clouds should be *short-lived*; they are expected to form stars and get dispersed on time-scales of a crossing time ($\sim 10^7$ yr) (e.g., Elmegreen 2000; Hartmann et al. 2001; Hartmann 2003). Star formation should thus be a fast, dynamic process (e.g. Hartmann 2001b; Elmegreen 2007; Dib et al. 2010).

However, no general consensus has yet been reached on the time scale of star formation; some theorists put forward the opposite view and claim that star formation is a "slow," quasi-static equilibrium process (e.g. Palla & Stahler 2000; Tan et al. 2006; Huff & Stahler 2007). A good way to test these competing theories is to measure the duration of the star formation process in a cloud by establishing the age spread of the YSO population. If the stars of a young cluster or a star forming region are placed in an HRD, they often display a substantial spread of luminosities at a given effective temperature. This apparent luminosity dispersion is sometimes directly interpreted as a spread in the ages of the individual stars and used to claim a long duration of the star formation process. For example, Palla & Stahler (1999) derived the isochronal ages for the stars in the Orion Nebula Cluster and constructed a histogram of the isochronal ages, from which they concluded that star formation

has been ongoing for about 10 Myr, and thus should be considered as a "slow" process (see Huff & Stahler 2007, for a follow-up study based on the same data). They also concluded that the star formation rate in the Orion Nebula Cluster, as well as in other star forming regions (Palla & Stahler 2000), has been accelerating to the present epoch, what they explain by global contraction of the parent clouds.

As demonstrated later in this paper, the interpretation of the ages derived from an HRD requires a detailed consideration of the effects of the observational uncertainties, which can easily mimic substantial age spreads in situations when in fact no age spread is present. Before discussing and illustrating this in more detail in Section 4, I summarize some basic properties of YSOs that are required to understand the origin of the observational uncertainties.

3 PROPERTIES AND EVOLUTION OF YSOS

Observations of YSOs started in the year 1852, when J. R. Hind discovered a faint nebula near the star T Tauri and found it to be strongly variable (see Hind 1864). Joy (1945) discovered further similar objects and defined the class of "T Tauri stars," based on the characteristics of rapid photometric variability, association with dark clouds, spectral type F or later, and the presence of emission lines (most notably Hα) in the optical spectrum. The nature of these objects was initially unclear, but further investigations (e.g. Herbig 1946; Joy 1949; Herbig 1950) lead to the recognition that T Tauri stars represent very young low-mass ($\leq 2\,M_{\odot}$) stars, in the earliest phase accessible to optical observations (Herbig 1957). Today it is known that the emission lines and the observed variability are mainly related to ongoing accretion of circumstellar material onto the star. While the proto-typical T Tauri stars show quite strong emission lines ($W(\mathrm{H}\alpha) \geq 10$ Å), many similar objects were found with a weaker or absent emission line; these were denoted as "weak-line T Tauri stars" and are thought to represent a slightly later evolutionary stage, where accretion has dropped to very low levels.

Young stars with higher masses ($2\,M_{\odot} \leq M \leq 8\,M_{\odot}$) were recognized some years later. The class of Ae/Be stars was first defined by Herbig (1960) as stars of spectral type earlier than F0 with emission lines, which lie in obscured regions and illuminate bright reflection nebulosity. Later, Strom et al. (1972) provided evidence that they are pre-main-sequence in nature.

The formation of high-mass stars ($M \geq 8\,M_{\odot}$) is not yet fully understood (see discussion in Zinnecker & Yorke 2007). Due to their very rapid evolution, massive stars do not have an observable PMS phase. They are already in the main-sequence stage as soon as they become accessible to optical/infrared observations.

In the 1970s, the advent of infrared observations (see Rieke 2009, for a historical overview) lead to the detection of many optically invisible infrared sources in dark clouds. It was soon clear that these embedded objects represent the progenitors of the T Tauri stars. The fast increase in infrared detector sensitivity and the observable wavelength range (mainly due to the space based observatories) lead to a strong boost in observations of YSOs during the last few decades.

3.1 Phases of Evolution

The evolution from a molecular cloud core to a zero-age main sequence star comprises a huge increase in density and temperature and proceeds via a number of steps. These steps correspond to a sequence of evolutionary phases with characteristic properties. One can distinguish the following main stages in the formation and evolution of YSOs:

1. **Pre-stellar core**: the collapse of a dense core marks the start of the star formation process. The moment in time when the core becomes optically thick with respect to its own radiation can be used to define the start of the life of the star, i.e. its zero age (see Wuchterl & Tscharnuter 2003).
2. **Collapse Phase**: the gravitational collapse of the core leads to the formation of a central protostar on timescales of just a few thousand years. Initially, the protostar contains only a small

fraction of the total core mass; most mass still resides in the collapsing envelope. As the dense envelope absorbs all the emission from the central protostar in this phase, it is usually impossible to observationally determine any stellar parameters.

3. **Protostar Phase**: the requirement of angular momentum conservation prevents the (initially very extended) circumstellar envelope from collapsing directly to the protostar; instead, a torus-like flattened structure forms, which quickly (within about 100 000 years or less) evolves into a circumstellar disk, from which the protostar accretes mass. As soon as most of the material in the envelope has collapsed onto the disk, the central protostar becomes observable at infrared wavelengths. In the theory of Palla & Stahler (1999) this moment in time is defined as the "birth" of the star. The spectral energy distributions of these objects are dominated by the infrared excess emission caused by the disk and envelope and peak at far-infrared wavelengths. The photospheric emission from the central protostar is still strongly obscured (and thus usually undetectable) at optical wavelengths, but the flux in the mid- and near-infrared range is sometimes high enough to allow the detection of photospheric spectral features in sensitive observations (e.g., Connelley & Greene 2010). Such infrared spectra provide the first opportunity to obtain reliable information about the basic stellar parameters of the YSO and place the object onto the HRD.
4. **Classical T Tauri star**: in this phase, the central stellar object has already attained most ($\gtrsim 90\%$) of its final mass, but is still surrounded by an optically thick circumstellar disk. The star continues to accrete matter from the disk, although usually at much lower rates than in the protostellar phase. These accretion processes are thought to be responsible for the strong emission lines (in particular Hα) that are a characteristic of the classical T Tauri stars. Photospheric emission from the young star is now rather easily observable and allows determining the luminosity and effective temperature of the central young star, but the spectral energy distribution still shows a strong infrared excess that is caused by the warm dust in the disk. On timescales of a few Myr, some fraction of the circumstellar matter is accreted onto the central young star or accelerated outwards in a jet or outflow, another fraction is turned into (proto-)planets, whereas the largest part is dispersed by the stellar UV and X-ray irradiation of the disk (see Ercolano et al. 2009).
5. **Weak-line T Tauri star**: after a few million years (at most about 10 Myr, see Briceño et al. 2007), almost all of the original gas and dust in the circumstellar disk has been dispersed. Some stars in this stage show still low levels of infrared excess emission, caused by thin remnant circumstellar disks, but the accretion rates have dropped to very low values. As a consequence, the emission lines are much weaker or completely absent in this phase.
6. **Pre-main sequence star**: after about $5 - 10$ Myr, the original protoplanetary disk is usually completely dispersed. The spectral energy distribution shows only photospheric emission from the young star. The star evolves with constant mass along its PMS track until it reaches the zero age main sequence (ZAMS). These disk-less young stars are often identified by their strong coronal X-ray activity (e.g. Casanova et al. 1995; Preibisch et al. 1996, 2011a), chromospheric activity (e.g. Herbig 1954; Wilking et al. 1987; Herbig 1998), the presence of lithium (Li) in the photosphere (e.g. Walter et al. 1994; Preibisch et al. 2002), or by their low photospheric surface gravity (e.g. Slesnick et al. 2008), or by their strong variability (e.g. Briceño et al. 2005). Some of these older PMS stars are surrounded by so-called "debris disks," that cause a far-infrared excess in the spectral energy distribution. In contrast to a protoplanetary disk, where most ($\sim 99\%$) of the mass is in the gas component, debris disks contain no significant amounts of gas but consist exclusively of (rather large) dust grains. This dust is thought to be produced and constantly replenished by collisions between planetesimals, and in this sense a debris disks can be considered as a "second generation" disk (see Krivov 2010, for a review) and a signature of the planet formation process.

The youth of a star ends when it enters the main sequence. The PMS evolution time scale depends very strongly on stellar mass and ranges from just $\lesssim 0.1$ Myr for high-mass ($M \geq 8\,M_{\odot}$)

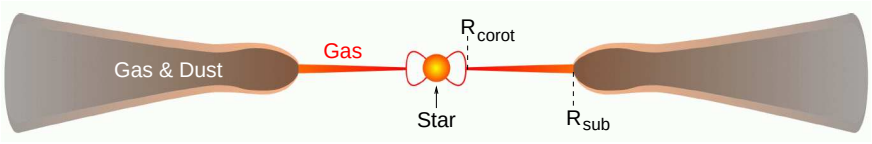

Fig. 1 Illustration of the structure in the inner regions of the circumstellar disk around a solar-mass young stellar object in the classical T Tauri stage. Typical sizes are: $R_* \sim 2\,R_\odot$, $R_{\rm corot} \sim 3{-}10\,R_*$, $R_{\rm sub} \sim 0.1$ AU ($\sim 10\,R_*$).

stars, and over ≈ 30 Myr for solar-mass stars, to several 100 Myr for very-low mass stars. The PMS lifetime of a low-mass star is thus much longer than the entire lifetime of a high-mass star (which is $\lesssim 5$ Myr for stellar masses $M \geq 35\,M_\odot$). In a co-eval population of stars, the low-mass stars are thus still in very early phases of their lives when the most massive stars have already reached the end of their lives. This is the reason why large star forming regions containing numerous very young low-mass stars in very early phases of their lives are often spectacularly marked by the final phases and supernova explosions of massive stars.

3.2 Basic Anatomy of a YSO in the Late Protostellar and T Tauri Phases

The circumstellar material around a YSO consists of gas and dust. Although the dust contains only $\sim 1\%$ of the total mass, it dominates the opacity of the circumstellar material. Thermal dust emission creates (nearly) all of the infrared excesses observed in YSOs. The gas, on the other hand, is mainly traced by spectral lines, which for YSOs are often found in emission. In most parts of the circumstellar disk, gas and dust are well mixed and coupled. This changes in the innermost disk regions, since the effective temperatures of young stars (typically in the range of 2500 to 10 000 K) are much higher than the sublimation temperature of the dust (around 1500 K for silicate grains). This implies that there is a minimum distance from the stellar surface where the dust grains can stay cool enough to survive in the solid phase. Inside of this so-called dust-sublimation radius, the stellar irradiation heats the dust grains above the sublimation temperature, causing them to evaporate. There is thus an inner dust-free zone, where the circumstellar material can only exist in the gas phase (see Fig. 1). Typical values of the dust sublimation radii range from ~ 0.1 AU for low-luminosity ($\sim 1\,L_\odot$) YSOs to ~ 10 AU for YSOs with high luminosities ($\sim 10^4\,L_\odot$). Since the opacity (per unit mass) of the gas is several orders of magnitudes lower than that of the original dust grains, the inner gas disk is usually assumed to be transparent (optically thin) to the starlight, while the outer dust disk is optically thick. However, recent results from infrared long-baseline interferometry (see Kraus et al. 2010) showed that in some YSOs the near-infrared emission seems to be dominated by radiation emerging from an optically thick inner gaseous disk (e.g. Kraus et al. 2008b), as predicted by theoretical models for objects with sufficiently high accretion rates (Muzerolle et al. 2004). A more detailed discussion of these aspects can be found in the recent review of Dullemond & Monnier (2010).

The accretion of matter from the circumstellar disk onto the central star is thought to be magnetically controlled. According to the magnetospheric accretion model (see Bouvier et al. 2007), stellar magnetic field lines connect the stellar surface to the surrounding disk. This leads to a truncation of the disk at or near the co-rotation radius, i.e. the radius where the Keplerian angular velocity of the disk matches the stellar angular velocity. Typical values for the co-rotation radius are a few ($\sim 3-5$) stellar radii, depending on the rotation period of the star. The magnetic field lines connecting the disk to the star produce a complex 3D system of "accretion funnels" that channel the accretion flow to

the stellar surface (see Romanova et al. 2008). The gas in the accretion funnels reaches free-fall velocities of several 100 km s^{-1} and finally generates shocks at the (proto-)stellar surface. This shock produces the UV and optical excess emission that is often seen in accreting YSOs (e.g., Gullbring et al. 2000) and can also produce observable amounts of X-ray emission under favorable circumstances (e.g., Brickhouse et al. 2010). It is often assumed that the hot gas falling down in these accretion funnels is the main source of the strong hydrogen emission lines typically observed in accreting YSOs. In particular, the Brackett-γ (Brγ) 2.166 μm line is considered as an accretion tracer, since the line luminosity $L_{\mathrm{Br}\gamma}$ was found to be well correlated with the mass accretion luminosity L_{acc} determined from UV veiling. This empirical $L_{\mathrm{Br}\gamma}$ versus L_{acc} relationship is often used to estimate accretion rates of YSOs (e.g. Garcia Lopez et al. 2006). However, recent observations with the technique of infrared long-baseline interferometry have shown that in some stars part of the line emission is caused by other processes, presumably stellar winds and outflows (Kraus et al. 2008a).

3.3 Variability in YSOs

Strong variability across all wavelength regimes is a characteristic of YSOs. This variability is a major source for uncertainties in the measured luminosities of YSOs that are usually derived from the observed fluxes in optical/infrared bands. Since these variability-related luminosity uncertainties represent a fundamental limit to the accuracy of age estimates for YSOs (see next section), I will discuss the different mechanisms that contribute to this variability in some detail. Some fraction of the observed flux variations is caused by inhomogeneities on the rotating stellar surface or in the inner disk regions; before describing these rotation-related variations, the main physical mechanisms of variations in the luminosity of YSOs will be considered.

3.3.1 Variations of the accretion process

Temporal variations of the accretion rate can produce considerable variability of the total luminosity of a YSO. The gravitational energy of the material falling down in the accretion funnels is transformed into heat in shocks at the stellar surface and is finally radiated away from the stellar surface. The corresponding accretion luminosity can constitute a substantial fraction of the total luminosity of a YSO. For example, a solar-mass YSO accreting at a rate of $\dot{M} \sim 10^{-6}\,M_{\odot}$ yr^{-1} has an accretion luminosity of a few times the solar luminosity. Any variation of the accretion rate is thus expected to lead to a corresponding change in the luminosity of the YSO.

The accretion rates of YSOs are highest during the embedded protostellar phase and decrease to values around $\dot{M} \sim 10^{-7}\,M_{\odot}$ yr^{-1} at the end of the classical T Tauri phase. This temporal decrease is probably not a smooth, monotonic decay. Instead, extended periods of quiescent low accretion seem to be punctuated by short but intense accretion bursts, where the accretion rates increase substantially for periods of days to decades (see Vorobyov & Basu 2006). The most intense of these accretion bursts provide an explanation for the very strong brightening of FU Ori objects (Hartmann & Kenyon 1996), where the optical fluxes increase by several magnitudes. While such large amplitude accretion bursts are relatively rare, episodic variations of the accretion rate by factors of $\sim 2-3$ on timescales of days to months seem to be very common (see, e.g., Alencar et al. 2005). These variations are probably a natural consequence of the fact that accretion disks are turbulent. The turbulence is a fundamental requirement making accretion at the observed rates possible in the first place, since it is thought that the predominant form of disk viscosity originates from the magneto-rotational instability that drives hydromagnetic disk turbulence (Balbus & Hawley 1998). Variations in the accretion rate can be caused by the accretion of individual "parcels" of matter along one accretion funnel (see Orlando et al. 2011, for a numerical modeling of such processes). The sum of numerous individual accretion events leads to fluctuations in the total luminosity (and thus the observed brightness) of YSOs.

Finally, variations of the accretion rate can also lead to changes in the observed spectrum of the YSO. The emission from the hot accretion shocks adds a continuum component to the photospheric spectrum (the so-called veiling; see Gahm et al. 2008); this can shift the derived effective temperature towards higher values and lead to errors in the determination of the extinction from the observed spectral type and the photometric colors (see Chelli 1999).

3.3.2 Variations of magnetic activity

YSOs typically show very high levels of stellar magnetic activity that is conveniently traced by coronal X-ray emission. Numerous X-ray observations of star forming regions and young clusters have clearly established that the X-ray luminosities of YSOs are typically $\sim 10^3 - 10^4$ times higher than those for main-sequence stars of similar mass (e.g., Feigelson & Montmerle 1999; Getman et al. 2005; Preibisch et al. 2005). These high X-ray activity levels stay approximately constant during the first ~ 10 Myr, before they drop towards the much lower levels typical for main sequence stars and our Sun after several 100 Myr (see Preibisch & Feigelson 2005). The X-ray emission from young stars is highly time variable (e.g., Wolk et al. 2005; Getman et al. 2008). A considerable fraction of the total X-ray output is emitted during flares, where the X-ray luminosity increases quickly by factors up to several hundred and then decreases in an exponential decay phase on time-scales of several hours (see Benz & Güdel 2010, for an overview of flares).

The coronal activity of YSOs is thought to be rooted in similar processes as those responsible for the coronal emission in the case of our Sun. The solar magnetic activity is known to affect the "Solar Total Irradiance," i.e. leads to variations in the optical brightness of the Sun. Some part of this variability is related to the appearance and disappearance of surface features such as dark sunspots and bright faculae, and their rotation across the observed solar disk; these processes will be discussed with the rotation effects below. On longer timescales, between months and centuries, changes of the magnetic activity level of the Sun cause variations in the Solar Total Irradiance of about 0.1% (e.g. Withbroe 2009). Periods of increased magnetic activity are characterized by higher optical fluxes, because the light-blocking effect of the sunspots is over-compensated by the intensification due to bright faculae, plages, and network elements. On short timescales (minutes to hours), magnetic reconnection flares also cause changes in the optical and infrared emission from the Sun. These flares are generally associated with changes in the optical/infrared emission, the so-called "white-light flares." The recent study of Kretzschmar et al. (2010) showed that this optical emission contains a major fraction of the total energy released in the flare. Although the amplitudes of the optical/infrared variations related to magnetic activity are quite small in the case of our Sun, the highly elevated magnetic activity of YSOs should increase these effects by factors of $\sim 10^3 - 10^4$. Variations of the magnetic activity and large flares can thus provide a substantial contribution to the optical/infrared variability of YSOs.

3.3.3 Dynamical changes in the disk structure

As accretion disks are intrinsically turbulent, some level of fluctuations in the density structure will always be present. Variations of the accretion rate will also cause changes in the structure and density of the innermost disk regions (see Flaherty et al. 2011). These dynamical changes in the inner disk structure will cause wavelength-dependent variations in the observed optical/infrared fluxes. For example, if the density or scale-height of the innermost disk regions increases (e.g., due to a temporal increase in the accretion rate), the inner disk will absorb a larger fraction of the stellar light. The decrease of the direct stellar flux seen by a distant observer looking at the YSO at a high inclination angle (i.e. close to edge-on orientation) may be accompanied by an increase in the near-infrared excess emission from the (now higher) dust sublimation rim. Since the higher dust sublimation wall will shadow larger regions of the disk behind the inner dust rim, these parts of the disk will receive

less stellar radiation and cool down, causing a decrease of the mid-infrared disk emission. Anti-correlated near- and mid-infrared variability that may be explained by such a scenario has been seen in some YSOs (Muzerolle et al. 2009).

3.3.4 Rotation related variations

The rotation of the stellar photosphere and the inner disk regions of a YSO can cause variations of the optical/infrared flux via different mechanisms. One important factor is the dark star-spots on the rotating photosphere that can explain the periodic brightness variations seen in many T Tauri stars. Whereas the solar spots cover only a very small fraction of the Sun's photosphere and produce correspondingly small flux variations, the highly elevated magnetic activity of YSOs leads to the formation of much larger star-spots, that can easily produce rotational variations of a few tens of percent in the optical lightcurves. This periodic variability is the basis of most rotation period measurements of YSOs (e.g., Littlefair et al. 2005). For sufficiently bright stars, the method of Doppler imaging even allows the reconstruction of the spot morphology (Schmidt et al. 2005; Strassmeier 2006).

For some YSOs, the lightcurves provide evidence that the variations are caused by bright (rather than dark) surface features; these are interpreted as accretion shocks at the stellar surface that follow the rotation of the stellar photosphere (e.g., Bouvier et al. 1995).

Inhomogeneities in the circumstellar structure can also produce rotational brightness variations. One possibility is that a column of accreting gas rotates across the line of sight and occults parts of the stellar photosphere. If the disk around a YSO is seen at an high inclination angle (i.e. close to the "edge-on" direction), rotating inhomogeneities in the innermost disk regions can lead to variable shadowing of the light from the central star.

3.3.5 Total amplitude of variability

The stellar rotation produces photometric variations with typical amplitudes of $\sim$0.1–0.5 mag in the optical bands for T Tauri stars (e.g., Littlefair et al. 2005). Typical total (periodic and non-periodic) variability amplitudes for T Tauri stars are several tenths of a magnitude in the optical bands (e.g., Stassun et al. 2006). Much larger amplitudes are possible, but rare.

Considering the near-infrared bands (that are often used to estimate luminosities of obscured YSOs), the typical variability amplitudes are again a few tenths of a magnitude (e.g., Morales-Calderón et al. 2011). Surprisingly high levels of variability, with flux variations by a factor of about two or more, have been found in the $4 - 8\,\mu$m emission of some YSOs (Muzerolle et al. 2009).

4 DETERMINATIONS OF STELLAR AGES AND MASSES FROM AN HRD

4.1 PMS Evolutionary Models

During the PMS phase, the luminosity and effective temperature of a young star change strongly with time. This provides the basis of age and mass determinations by comparison to theoretical PMS evolutionary models. Frequently used sets of PMS evolutionary models are those of D'Antona & Mazzitelli (1994), Baraffe et al. (1998), Palla & Stahler (1999), and Siess et al. (2000). The recent models of Tognelli et al. (2011) are particularly useful for extragalactic regions with low metalicity. It is important to keep in mind that all these models are based on some simplifying assumptions and use more or less artificial initial conditions. It is still impossible to accurately model the full temporal evolution from a collapsing cloud core up to the arrival of the resulting star on the main sequence in a consistent way, because the important physical parameters change by many orders of magnitude during this process. For example, the density increases by some 20 orders of magnitude and the temperature by about 6 orders of magnitude. This prevents a coherent numerical modeling of the

full evolution sequence. In fact, most models do not consider the protostellar collapse and accretion phases but instead start from the rather arbitrary initial condition of a fully convective object with very large radius that is contracting and moves down the Hayashi line. As a consequence, all PMS models suffer from substantial uncertainties for very young objects, at ages less than about 1 Myr (see discussion in Baraffe et al. 2002).

Since the different models use different ingredients describing the stellar interior and different atmosphere models, the predicted PMS tracks as a function of stellar temperature and luminosity are not identical. However, the differences between the recent models are now relatively small, typically $\lesssim 20\% - 30\%$.

4.2 Measurements of the Stellar Parameters

The most reliable way to measure the stellar effective temperature is to derive the spectral type from optical spectroscopy. For optically faint, obscured YSOs, near-infrared spectroscopy can provide a good alternative (e.g., Luhman et al. 2005). If the spectra have sufficiently high quality, spectral types can be determined with an accuracy of about half a sub-type. In order to translate the spectral type into effective temperature, one has to take into account that the temperature calibration for PMS stars is not identical to the well established and widely used calibration for main-sequence stars, because the young PMS stars have larger radii and consequently lower surface gravities than main-sequence stars of the same spectral type. This issue is discussed in some detail in Luhman (1999), who established a temperature calibration for stars with ages of a few Myr that is compatible with the PMS evolutionary models of Baraffe et al. (1998). The temperatures in this calibration are intermediate between dwarf and giant temperature scales and about 20 – 100 K warmer than the corresponding main-sequence scale for M-type stars. In the ideal case, if the spectral type can be reliably determined with an accuracy of half a sub-type, the uncertainty of the effective temperature determination can be as low as ≈ 75 K.

The stellar luminosity is usually determined from optical photometry, a correction for the extinction, and the use of an appropriate bolometric correction factor. It should be noted that the bolometric correction is also sensitive to the surface gravity; the corresponding calibration uncertainties result in a minimum uncertainty of about 10% for the derived luminosities.

The mentioned uncertainties of ≈ 75 K in effective temperature and $\approx 10\%$ in luminosity represent lower limits. They can only be reached in the ideal case of YSOs that have no (or negligible amounts of) circumstellar material, very low extinction, very low variability, and for which high precision photometry as well as high signal-to-noise optical spectra are available. In such cases, the accuracy of the mass and age estimates derived from the HRD location is quite good. Hillenbrand & White (2004) studied several young stars in resolved multiple systems and found that the stellar masses determined from the HRD location agree within about 20% with the masses determined from measured orbital dynamics. Observations of eclipsing binary stars show that PMS models generally perform very well in predicting age differences of less than 5% for binaries with components more massive than $\sim 1\,M_{\odot}$ (Stassun et al. 2009). For lower mass systems, larger differences of the isochronal ages are sometimes present, presumably because magnetic activity inhibits convection and causes the stellar radii to be underestimated.

4.3 Uncertainties in the Measurement of the Stellar Parameters of YSOs

For most YSOs that are still surrounded by circumstellar material and/or embedded in the clouds of star forming regions and often quite faint at optical wavelengths, the uncertainties in the derived stellar parameters are substantially larger than the above mentioned ideal limits. One fundamental limit to the accuracy of the measured luminosities results from the photometry errors. Although these errors are usually very small (often $\lesssim 1\%$) for the brighter stars in a young cluster, the photometry

errors often amount to ~ 0.1 mag or more for the faintest stars in the sample. Beyond this, there are a number of other factors that contribute to, or even dominate, the deviations between true and inferred stellar parameters. The effects of the variability of YSOs have already been described above. Other important factors are:

• **Extinction correction**

In most star forming regions and young clusters, the individual stars suffer from different amounts of interstellar and circumstellar extinction, i.e. show "differential extinction." An accurate measurement of this extinction is often problematic. Even if the combination of stellar spectroscopy and multi-band photometry allows a reliable determination of the color-excess for each star, transforming this color-excess to extinction values requires knowledge of the extinction law (i.e. the exact wavelength dependence of the opacity). In many star forming clouds, the extinction law seems to differ from the standard interstellar extinction law (e.g., Povich et al. 2011), and this "anomalous" extinction law changes the relations between colors and the extinction (see Mathis 1990). The variations in the extinction law are most likely related to different grain sizes or shapes. For YSOs, where a significant part of the total line-of-sight extinction often originates from local circumstellar material (rather than from interstellar cloud extinction), it is very possible that each star has its own individual extinction law, which is set by the specific distributions of the sizes of grains in each individual circumstellar disk. In fact, there is direct observational evidence that grains of different sizes and compositions are present in different parts of the disks around young stars (see van Boekel et al. 2004), and this will affect the extinction law. These effects can easily lead to uncertainties of a few tenths of a magnitude in the derived extinction correction.

• **Excess emission**

Many YSOs show some level of excess emission from accretion processes, especially in the blue part of the optical spectrum. These excesses will affect the measured colors of the YSOs (in particular the $U-B$ or $B-V$ colors) and can cause an underestimate of the extinction, which will finally result in an underestimate of the stellar luminosity. The veiling of the optical spectrum caused by accretion-related excesses reduces the measured equivalent widths of spectral lines and can lead to errors in the determination of the spectral type. In the red and infrared parts of the spectrum, excess emission from circumstellar matter plays an important role. The infrared excesses can easily lead to serious over-estimates of the stellar luminosity, especially in cases where near-infrared photometry is used to determine the stellar parameters.

• **Unresolved binary systems**

It is well established that many young stars are members of binary or higher order multiple systems (see Duquennoy & Mayor 1991; Zinnecker & Mathieu 2001). Since the distribution of binary separations peaks around a few ten AUs (Raghavan et al. 2010), most of these multiple systems will remain unresolved and appear like single stars in conventional, seeing-limited observations of clusters at distances of $\gtrsim 100$ pc. The observed (combined) spectrum is usually dominated by the brighter, i.e. the primary component, and consequently, the derived spectral type is (close to) that of the primary star. The measured flux of the unresolved system, however, is the sum of the individual stellar fluxes. This causes an overestimate of the stellar luminosity by up to a factor of two. This effect is further increased by the fact that a companion that is cooler than the primary star also causes a color excess, i.e. the measured color of the binary system is redder than the color of the primary star. This causes the extinction to be overestimated and leads to an additional overestimate of the stellar luminosity.

• Inconsistencies due to non-simultaneous observations

Often, the spectroscopic and photometric observations of a YSO cannot be obtained simultaneously. In this case, it is possible that variability leads to inconsistencies in the data that may adulterate the derived stellar parameters. For example, changes in the photospheric star-spot coverage or the accretion rate during the time period between the individual observations can change the photometric colors and affect the derived extinction correction.

• Spread of individual stellar distances

Usually, the individual distances of the stars in a cluster cannot be measured and the mean distance is assumed for all stars. The corresponding error is very small in the case of compact clusters at distances beyond a few hundred pc. However, the distance spread can be quite significant in studies of very nearby and extended star forming regions (e.g., Taurus) or OB associations (e.g. de Bruijne 1999; Preibisch et al. 2002, for the case of the Scorpius-Centaurus OB association).

4.4 A Simulated HRD with Realistic Observational Uncertainties

In order to illustrate the influence of observational uncertainties on the locations of young stars in the HRD, I show here a simulation of an artificial data set of a young cluster. The input model is a cluster of 6000 stars with true masses between 0.1 and 7 $M_{\odot}$. The individual stellar masses have been randomly drawn from a distribution following the Kroupa (2002) field star IMF representation. The model cluster is **strictly co-eval***: all stars have exactly the same age of 3 Myr*. The PMS model isochrones from Siess et al. (2000) are used to determine the luminosity and effective temperature for each simulated star from its mass. If one could measure the effective temperature and luminosity of the stars without any error and would put these values into the HRD, all stars would, of course, lie exactly on the 3 Myr isochrone.

The observational uncertainties change this and cause the "observed" HRD location based on the measured parameters to deviate from the "true" position. For the following discussion, it is useful to explicitely distinguish between the *true parameters* of a star and the *inferred parameters* that are deduced from the observations and the corresponding HRD location, which will be denoted as *"isochronal" parameters* in the following text.

To simulate the effects of the observational uncertainties, I assume that an observer would calculate the bolometric luminosities of the observed stars from their I-band magnitudes. For the combination of the effects of stellar variability, photometry errors, and the uncertainties in the extinction determination, I add a random variable taken from a normal distribution with $\sigma = 0.15$ mag to the intrinsic I-band magnitude of each star. Furthermore, I assume that 50% of the stars are unresolved binary systems that have a flat mass-ratio distribution. The I-band flux of each simulated companion is then added to the flux of the primary star. In order to simulate the uncertainties in the temperature measurement, the effective temperature value of each simulated star is changed by adding a normally distributed value with $\sigma(\log T_{\rm eff}) = 0.005$ dex (corresponding to a temperature error of $\Delta T \approx 50$ K at $T = 4000$ K). Finally, for plotting the HRD, I assume that the observing completeness drops with mass from 100% for $M > 0.25\,M_{\odot}$, via 80% for $0.25 \leq M < 0.2\,M_{\odot}$, 60% for $0.2 \leq M < 0.15\,M_{\odot}$, to 40% for $M < 0.15\,M_{\odot}$.

Figure 2 shows the resulting HRD. The pluses show the simulated stars with the added uncertainties. The distribution shows a scatter of about 0.6 dex in luminosity for any given effective temperature. This scatter mimics a considerable age spread. Most stars appear above their true position in the HRD, i.e. their isochronal age is smaller than the true age; this is a consequence of the unresolved binary companions. Note that the assumed observational uncertainties in this simulation are not unrealistically large. Some factors, such as the uncertainty of the extinction correction due to binary companions or excess emission, have not been included. Therefore, real data sets of YSOs in

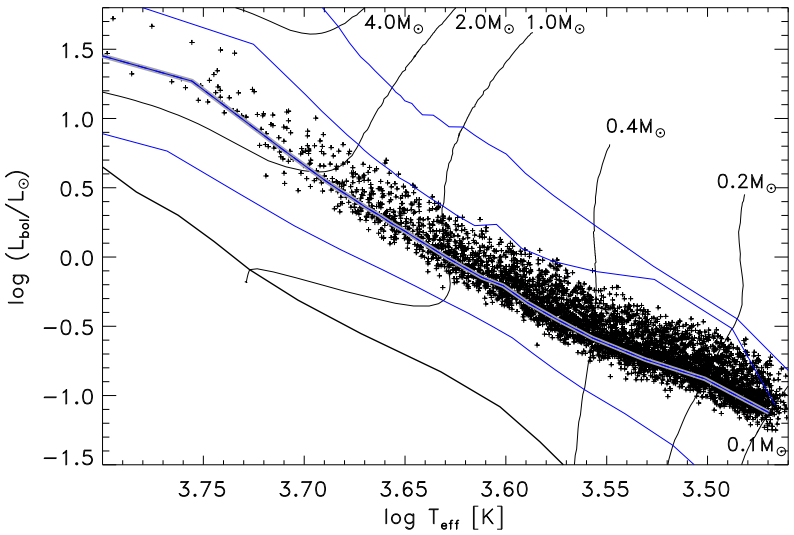

Fig. 2 Monte-Carlo simulation of an HRD for a perfectly co-eval model cluster of 6 000 stars with identical ages of 3 Myr and a distribution of masses between 0.1 and 7 $M_\odot$ according to the Kroupa (2002) IMF. The black lines show evolutionary tracks for different stellar masses according to the Siess et al. (2000) models. The blue lines show the isochrones for ages of 0.3, 1, 3 and 10 Myr, and the ZAMS (*thick black line*). The pluses show the positions of the stars after including the simulated observational uncertainties described in the text, while the thick gray line marks the theoretical 3 Myr isochrone.

star forming regions will tend to have even somewhat larger uncertainties, and this will increase the scatter seen in the HRD even more.

4.5 Isochronal Ages and Age Spreads Derived from the HRD

Here I consider in more detail how the observational uncertainties affect the distribution of derived isochronal ages. To this end, I focus on the errors of the observationally determined luminosities. Two simulations were performed for the case of a star with a mass of $0.5\,M_\odot$, assuming a true age of 2 Myr in the first case and 5 Myr in the second case. The observational effects of stellar variability and unresolved binary companions were simulated as described above and used to compute the observed luminosity for each of the 10 000 model stars. Then, the PMS models of Siess et al. (2000) were used to determine the isochronal age corresponding to the simulated observed luminosity. The resulting distributions of isochronal ages are shown in Figure 3.

The statistics of the distribution of isochronal ages for the true age of 2 Myr are as follows: The mean value of the isochronal ages is 1.73 Myr, the median value is 1.71 Myr, and the standard deviation is 0.50 Myr. The central 80th percentile of the isochronal ages ranges from 1.09 Myr to 2.39 Myr; the "80% isochronal age spread" is thus $2.39 - 1.09 = 1.3$ Myr, or 76% of the median isochronal age.

The distribution of isochronal ages for the true age of 5 Myr has a mean value of 4.11 Myr, a median of 4.06 Myr, and a standard deviation of 1.40 Myr. The central 80th percentile ranges from 2.30 to 5.93 Myr; the "80% isochronal age spread" is thus 3.6 Myr, or 90% of the median isochronal age.

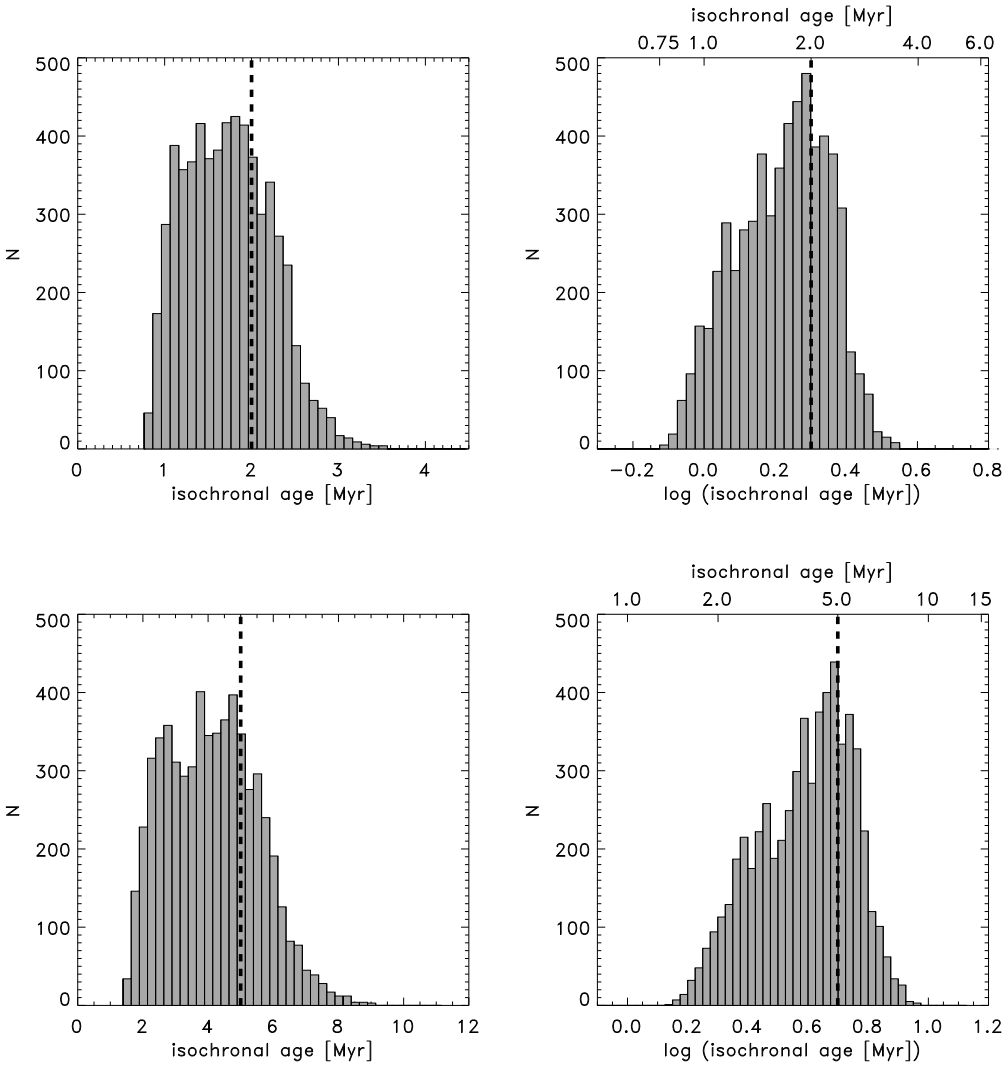

Fig. 3 Distribution of the isochronal ages found in the simulation of the observational uncertainties as described in the text. The thick dashed lines mark the true ages, which are 2 Myr for the upper row and 5 Myr for the lower row. Each distribution is shown twice, first with a linear age axis and binning (*left*) and then with a logarithmic age axis and binning (*right*).

If one would ignore the effects of the observational uncertainties and (wrongly) assume the derived isochronal ages to represent the true ages, one would erroneously infer from these age histograms the presence of a substantial age spread. In fact, there is no age spread at all, and the spread of isochronal ages is just the effect of the observational uncertainties.

A particularly interesting feature of the distribution of isochronal ages is the roughly exponential drop in the number of stars with increasing isochronal age that can be seen in the histogram with the linear age axis for ages above the median value. Such a shape can easily be misinterpreted as a signature of an “increasing star formation rate” and lead to erroneous claims that star formation has been accelerating over time.

The conclusions from this simple simulation are as follows: First, the observed spread of isochronal ages derived from an HRD must not be confused with a physical age spread; **it is always just an upper limit to a possible age spread**. The observed scatter is always substantially larger than the effect of the (usually small) photometry errors, because it is usually dominated by the effects of variability and unresolved binary companions. Second, any claim of a physical age spread requires a detailed consideration of all observational uncertainties in the data set. It is necessary to show that the spread of isochronal ages is significantly larger than the effects of the uncertainties. If this cannot be demonstrated, the data are consistent with the assumption that all stars have the same age, i.e. there is no age spread. Third, an approximately exponential decrease of the number of stars per linear age bin does not automatically provide evidence for an "increasing star formation rate." Such a pattern may just be the expected signature of the uncertainties in the distribution of isochronal ages.

5 AGE ESTIMATES DERIVED FROM COLOR-MAGNITUDE DIAGRAMS

Sometimes, especially in studies of more distant star forming regions, it is not feasible to obtain optical or near-infrared spectra of all individual stars. The comparison to the PMS models is then only based on photometric data and performed with color-magnitude diagrams (CMDs). Since the theoretical PMS models predict the colors and magnitudes of young stars as a function of age and mass, this procedure is, in principle, quite similar to the analysis of an HRD. The analysis of CMDs is a very well established technique and can provide reliable results in the case of clusters with ages of at least ~ 5 Myr, where the main-sequence turnoff and the locations of the evolved massive stars yield good age constraints.

However, for studies of very young low-mass PMS stars in star forming regions, the analysis of a CMD faces several serious difficulties. One fundamental problem is that, without spectroscopic information, the extinction of the individual stars cannot be reliably established from the observed colors, if the age of the stars is unknown. This causes a severe ambiguity between stellar temperature and extinction. Attempts to estimate individual stellar extinctions from color-color diagrams do often yield plurivalent results, and are generally not very reliable because the circumstellar matter around YSOs causes their intrinsic colors to differ from those of main-sequence stars by unknown amounts. Since most YSOs suffer from significant levels of extinction, partly due to circumstellar material and partly from surrounding cloud material, this constitutes a very serious problem.

In cases where infrared (rather than optical) photometry is used to construct the CMD, these problems are even more pronounced due to infrared excesses from circumstellar matter. The combined effects of emission, absorption, and scattering of light by circumstellar matter can shift a YSO in any direction in the CMD, depending on the details of the circumstellar matter distribution (e.g., Whitney et al. 2003; Cieza et al. 2005). These effects can easily lead to errors up to about a factor of 10 if one tries to estimate the mass and age for individual YSOs from a CMD.

In Figure 4, these effects are demonstrated in a simulation of the near-infrared J versus $J - H$ CMD for a co-eval population of stars with an age of 3 Myr. The plots show step by step how the effects of variability and unresolved binaries, differential extinction, and finally infrared excesses shift the observed colors and magnitudes from the original stellar values. This simulation demonstrates the very substantial scatter in the CMD of this co-eval population of YSOs.

The "knee" of the isochrones in the color range between $J - H = 0$ and $J - H \approx 0.4$ provides the best age diagnostic power in such a CMD. However, the simulation shows that the observational uncertainties produce an almost uniform distribution of simulated stars between the 1 Myr isochrone and the ~ 5 Myr isochrone, which mimics a large apparent age spread in this actual co-eval population. This shows that any age estimates for low-mass YSOs derived from a CMD suffer from substantial uncertainties. Age spreads can only be detected in a CMD if they are several times larger than the true age.

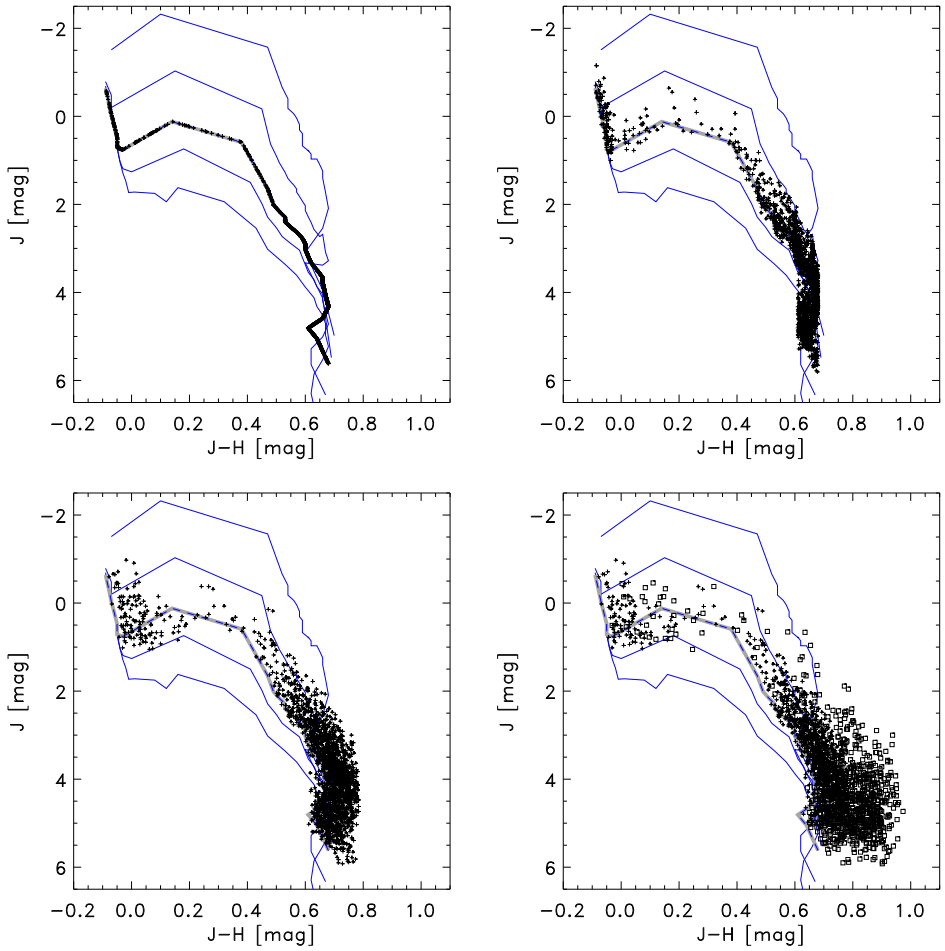

Fig. 4 Different stages of the Monte-Carlo simulation of a near-infrared color-magnitude diagram for a perfectly co-eval cluster of 6 000 stars with identical ages of 3 Myr and a distribution of masses between $0.1\ M_{\odot}$ and $7\ M_{\odot}$ according to the Kroupa (2002) IMF. The blue lines show the isochrones for ages of 0.3, 1, 3, 5 and 10 Myr according to the Siess et al. (2000) models. The "true" isochrone for 3 Myr is emphasized by the thick gray line. The crosses show the positions of the simulated stars. The upper left panel shows the theoretically expected magnitudes of the simulated stars. In the upper right panel, the effects of unresolved binaries and the stellar variability (as described in Sect. 3) is included. In the lower left panel, the effect of differential extinction (following a uniform distribution in the range $A_V = [0 - 1]$ mag) is added. In the lower right panel I added excess infrared emission to 20% of the stars (marked by open boxes), assuming a uniform distribution of $\Delta(J - H)$ values in the $[0 - 0.2]$ mag range according to Meyer et al. (1997).

6 FURTHER REASONS FOR APPARENT LUMINOSITY /AGE SPREADS IN HRDS OR CMDS

Besides the observational uncertainties in the stellar parameters discussed so far, there are further factors that can cause a spread of the measured luminosities (or magnitudes) and can thus mimic an age spread in the HRD or CMD.

6.1 The Effect of the Accretion History

Temporal variations of the accretion rate not only have an instantaneous effect on the total luminosity of a YSO, but can also have a more long-lasting effect on the global evolution of the stellar parameters. The temporal evolution of the accretion rate is an important input parameter of the theoretical PMS evolution models. Most models assume (as an initial condition) that accretion has essentially ceased and the YSOs contract at constant mass. If, however, accretion is still ongoing during the optically visible phases of a YSO, it will affect the evolution of the internal stellar structure. Consequently, the evolutionary track of a YSO in the HRD will depend on the temporal evolution of the accretion rate (see, e.g., Siess et al. 1999; Tout et al. 1999).

The study of Baraffe et al. (2009) investigated the effects of intermittently variable accretion rates on the PMS evolution. Assuming that long phases of quiescent accretion with rates of $\dot{M} < 10^{-6}\,M_{\odot}\,\mathrm{yr}^{-1}$ are punctuated by a few thousand year-long episodes with accretion rates of $\dot{M} \geq 10^{-4}\,M_{\odot}\,\mathrm{yr}^{-1}$; their models produced a considerable spread of luminosities in a co-eval stellar population. They found that a population of stars with identical ages of a few Myr may be wrongly interpreted to have an age spread of up to ~ 10 Myr if the isochronal ages are assumed to be identical to the true ages. Even with more moderate amplitudes of the accretion episodes, apparent age spreads of a few Myr can be produced in this way. Observational evidence for such accretion-history related effects on the luminosity evolution of YSOs has been reported by Littlefair et al. (2011). It is therefore highly likely that a considerable part of the observed luminosity spreads in observed HRDs of star forming regions is due to variable accretion rates.

In another study, Baraffe & Chabrier (2010) showed that non-steady accretion will also produce substantial variations in the level of Li depletion in PMS stars of a given age. This is relevant because, until recently, measurements of Li abundances in PMS stars were often assumed to provide reliable age diagnostics. Previous studies of some nearby star forming regions had identified significant numbers of apparently Li-depleted stars which were thus assumed to be considerably older than the bulk of the young stellar population (Martín 1998; Palla et al. 2007; Sacco et al. 2007). These results were sometimes used to claim the existence of large age spreads and long timescale for the star formation process. However, new and more accurate determinations of the Li abundances showed that the number of significantly Li-depleted stars is greatly reduced with respect to earlier results (e.g. Sestito et al. 2008, for the case of the Taurus region). It was also found that magnetic field intensification of the Li 6708Å doublet can produce a considerable scatter of the inferred Li abundances, which could make stars appear millions of years younger than they actually are (Leone 2007). The observed scatter of Li abundances does, therefore, not necessarily provide support for claims of large age spreads.

6.2 Alternative Explanations for the Presence of Apparently Older Stars in Young Clusters

Some young clusters or star forming regions seem to contain a number of stars with substantially older ages than the bulk of the young stellar population. One example is the Orion Nebula Cluster, for which the HRD presented by Hillenbrand (1997) shows a few dozen stars roughly aligned with the 10 Myr isochrone, whereas the large majority of members (~ 500 stars) has much younger ages of around 1 Myr. It is sometimes claimed that this apparently older population would demonstrate an extended period of star formation. However, there are also a number of alternative explanations.

6.2.1 YSOs with edge-on disks

One possibility is that these apparently older stars are in fact YSOs with circumstellar disks that are seen (nearly) edge-on. In such a case, the disk will block the direct light from the stellar photosphere from our view, and what we see is scattered stellar light at the upper and lower edge of the disk.

Several examples of such edge-on disks have been detected in high-resolution observations of YSOs (Stapelfeldt et al. 1998; Zinnecker et al. 1999; Wolf et al. 2003; Preibisch et al. 2011b).

If the objects are close enough and the observations have sufficient angular resolution, such objects are easily identified because the distribution of scattered light from the upper and lower disk rim is intersected by a prominent central dark lane that represents the shadow of the disk and hides the central star. However, in seeing-limited observations of more distant star forming regions, such objects can usually not be spatially resolved and thus their nature cannot be recognized. The only noticeable signature is a particularly low brightness, because nearly all the stellar light is blocked from our view. Consequently, the stellar luminosity derived from the observed fluxes strongly underestimates the true luminosity, and this can explain the peculiar HRD positions of such objects.

6.2.2 Foreground stellar populations

Confusion by foreground stellar populations is another possibility. The Orion Nebula Cluster again provides a good example. It has long been known (but apparently is not general knowledge) that the subgroup 1c of the Ori OB1 association is located directly in front of the Orion Nebula Cluster (see Blaauw 1964; Brown et al. 1994; Bally 2008). Since OB associations generally contain extensive populations of low-mass stars (Briceño et al. 2007), and the members of the Ori OB1c group have ages of a few (~ 4) Myr, some of these older Ori OB1c members will be seen in projection in the area of the Orion Nebula Cluster and contaminate the HRD. Note that the study of Fűrész et al. (2008) reported direct evidence for a foreground population of older stars in front of the Orion Nebula Cluster.

6.2.3 Field stars captured during the collapse of the clouds

Even if it can be shown that the older stars are actually genuine members of the young cluster (e.g., by kinematic investigations), this still does not prove that a large age spread is present. An interesting alternative explanation has been suggested by Pflamm-Altenburg & Kroupa (2007). They show that a collapsing pre-cluster cloud can capture older stars from the surroundings during its formation phase. Therefore, the presence of some (apparently) older stars in a young cluster does not necessarily imply that the star formation in this region occurred over a prolonged period.

7 STELLAR PARAMETERS DERIVED FROM BROAD-BAND SPECTRAL ENERGY DISTRIBUTIONS

In the absence of spectroscopic information, another possible way to obtain information about the stellar parameters of a YSO is by modeling the broad-band spectral energy distribution (SED) with radiative transfer simulations. For example, the SED models of Robitaille et al. (2006) for YSOs with disks and envelopes are often used to determine the stellar and circumstellar parameters from multi-band photometry. This is very useful to identify YSOs by their infrared excesses and to estimate their luminosities and the amounts of circumstellar material. However, it has to be emphasized that these SED models are often highly ambiguous; the stellar and circumstellar parameters are often only poorly constrained because the models show a high degree of degeneracy (e.g. Men'shchikov & Henning 1997). In particular, the resulting effective stellar temperature is often very uncertain, especially if only infrared photometry is available.

The problems of stellar parameters derived from such SED fits are well illustrated by the case of the so-called "Flying Ghost Nebula," an embedded YSO in the cluster IC 348. The modeling of photometric data suggested the object to be a $4\,M_{\odot}$ B-type star (Boulard et al. 1995). A few years later, spectroscopy by Luhman et al. (1998) showed that the object is in fact an M0.5 star with a mass of about $0.5\,M_{\odot}$. Any attempts to estimate ages of individual YSOs from SED models are prone to similarly large uncertainties.

8 CONCLUSIONS

HRDs and CMDs are very useful tools to infer information about the stellar ages and age spreads in the populations of star forming regions or young clusters. However, the interpretation of the derived isochronal ages requires awareness and a careful consideration of the observational uncertainties.

8.1 Important Considerations for the Interpretation of Isochronal Age Distributions

1. The inevitable observational uncertainties cause a deviation of the measured stellar luminosity and temperature from the true values. If the objects are placed into an HRD, these deviations produce a scatter that is usually considerably larger than the contribution of the photometry errors alone.
2. If the isochronal ages are erroneously assumed to represent the true ages, this can lead to misdiagnosed and strongly over-estimated age spreads. **The spread of isochronal ages** derived from an HRD **is always just an upper limit to a possible age spread**. For a perfectly co-eval population of stars, the expected spread of isochronal ages due to these uncertainties is about as large as the mean isochronal age, i.e. it amounts to several Myr for clusters with a true age of a few Myr.
3. Underestimating the uncertainties can lead to gross overestimates of the age spread. Any claim of age spread must be associated by the proof that the observed spread of the isochronal ages is larger than the spread caused by the observational uncertainties. The unavoidable intrinsic scatter of the isochronal ages makes it very difficult, often impossible, to detect and measure age spreads of less than a few Myr.
4. If the isochronal ages are plotted in a histogram with a linear age scale, the observational uncertainties will naturally produce a pattern of an approximately exponential drop in the number of objects per isochronal age bin for ages above the mean isochronal age. Such a pattern can easily be misinterpreted as an accelerating star formation rate.
5. Age estimates derived from a CMD often suffer from substantially larger uncertainties due to the lack of spectroscopic information. The problem is particularly severe if infrared (rather than optical) photometry is used and for very young clusters, in which most YSOs show infrared excesses and are affected by significant differential extinction from the surrounding clouds. While it is still possible to derive a (rough) estimate of the mean age of a stellar sample, meaningful information about a possible age spread is very hard, often impossible, to obtain. The age diagnostic power of CMDs improves strongly for ages of $\gtrsim 5$ Myr, when most YSOs have dispersed their circumstellar material and the surrounding clouds are also largely removed.

8.2 On Literature Results on Ages and Age Spreads in Young Stellar Populations

As mentioned above, any claim of an age spreads requires a proof that the scatter of isochronal ages is significantly larger than the effect of the full range of observational uncertainties. The best way to show this is to perform a detailed modeling of the specific observational uncertainties before interpreting the HRD (or CMD). The studies of Hennekemper et al. (2008) and Da Rio et al. (2010) provide examples for such a careful analysis. However, sometimes the effects of the observational uncertainties are not fully appreciated and seriously underestimated. This can easily lead to dubious results (see also the discussion in Hillenbrand et al. 2008). In particular, the observed luminosity spread in an HRD is sometimes misinterpreted as a genuine age spread and used to claim a prolonged period ($\gtrsim$ 10 Myr) of star formation. There are numerous examples of studies where a new and more careful data analysis leads to serious revisions or rejections of previous claims of this kind. To mention just two examples, I refer to the study of the young cluster NGC 3293 by Baume et al. (2003) that led to a correction of previous claims about the stellar ages, and to the new results of

Currie et al. (2010) for h and χ Persei, which clearly refute earlier claims of different ages and large age spreads for the double cluster.

8.3 Age Spreads versus Age Differences

As a final point of this discussion I would like to emphasize that a careful definition of the stellar sample is of essential importance for a meaningful interpretation of the age distribution. The concept of an age spread only makes sense if one considers *a coherent population of stars that have formed together*; only in this situation does the observed age distribution contain information about the star formation process.

It is well known that many large star forming regions consist of several *distinct stellar populations* in separate clusters or groups, that often have different ages. Besides the already mentioned OB associations Sco OB2 and Ori OB1, which show age differences of a few to several Myr between the different sub-groups (Bally 2008; Preibisch & Mamajek 2008), the Carina Nebula Complex provides another good example, as it contains several individual clusters with ages ranging from $\lesssim 1$ to ~ 8 Myr (see Smith & Brooks 2008; Preibisch et al. 2011c). These examples illustrate that large star forming regions generally seem to have complex star formation histories, typically involving a sequence of individual star formation episodes that created the individual sub-groups or clusters. This is often related to the feedback effects of the massive stars on the surrounding (remnant) molecular clouds. Expanding HII regions, wind-blown bubbles, and evolved supernova-shock waves can compress clouds and thereby trigger the formation of new generations of stars (e.g., Reach et al. 2004; Cannon et al. 2005; Oey et al. 2005; Preibisch & Zinnecker 2007; Deharveng et al. 2009; Gritschneder et al. 2010; Zavagno et al. 2010).

In such a situation it is very important to distinguish between the *age difference* between the individual parts of a complex, and the *age spread* within each of these individual clusters or subgroups; these are two conceptually different quantities. This distinction can be relatively simple in the case of nearby star forming regions that are seen under a favorable viewing angle, so that the

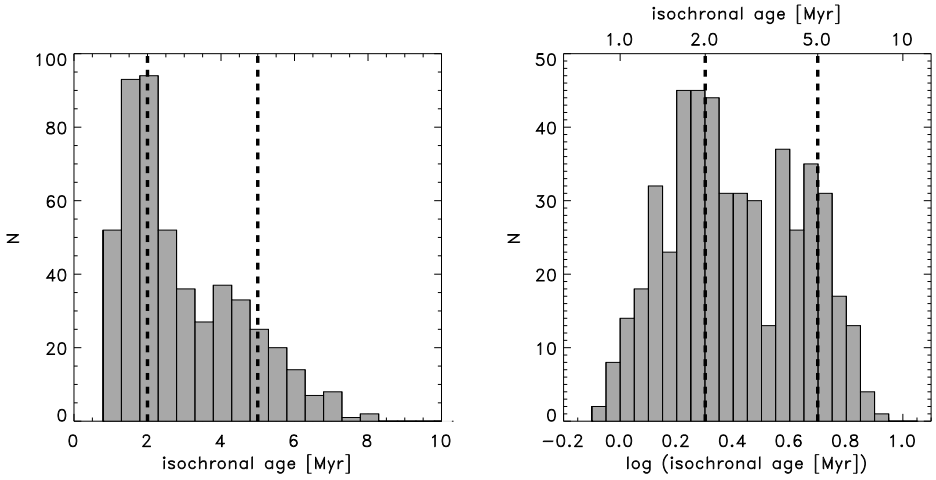

Fig. 5 Distribution of isochronal ages found in the simulation of a sample consisting of 250 stars with true ages of 2 Myr and 250 stars with true ages of 5 Myr. The simulation of the observational uncertainties and their effect on the isochronal ages were done as described in Sect. 4.5. The left plot shows the histogram with a linear age axis and binning, and the right plot with logarithmic age axis and binning. The thick dashed vertical lines mark the true ages of the two sub-samples.

different stellar groups can be easily discerned. However, in observations of distant star forming complexes it is often impossible to reliably distinguish (or even recognize) the different populations, in particular in cases where these are projected onto each other. An HRD (or a CMD) constructed from all detected stars in a given field-of-view will naturally show a wide age distribution because all the stars in the different sub-groups with different ages are mixed together.

However, for the understanding of the star formation process it would be very important to distinguish between a scenario of a slow continuous star formation process (that would produce a large age spread in a single stellar population) and the alternative scenario of a temporal sequence of individual short star formation episodes (where the individual populations can have age differences of several Myr but small internal age spreads). Unfortunately, the spread of isochronal ages derived for co-eval stellar populations makes this distinction very difficult and often impossible.

In order to illustrate this, I show in Figure 5 histograms of isochronal ages extracted from simulated observations of a cluster consisting of two equally large sub-populations with different ages. Half of the stars has an age of 2 Myr, while the other half has an age of 5 Myr. The simulations of the observational errors and the determination of the isochronal ages were performed as described in Sect. 4.5, i.e. are based on the assumption that spectral types and luminosities have been measured for each star and isochronal ages are derived by comparison to theoretical PMS evolution tracks in an HRD. In order to reflect the typical size of spectroscopically observed stellar samples in star forming regions, the simulation uses 500 stars. The resulting histogram of the isochronal ages provides only a marginal hint for the presence of two individual peaks in the age distribution. It is not possible to reliably discern between the (correct) model of two episodes of star formation and the (wrong) model of a more continuous and accelerating star formation process.

8.4 Final Comments on Age Spreads

The main message of this paper is that age spreads are difficult to measure in an HRD or a CMD and are very easily overestimated. This does, of course, *not* mean that age spreads (or increasing star formation rates) do not exist. From a physical point of view, some amount of age spread must clearly be present, since it is impossible that all stars in a cluster formed at exactly the same moment. A more meaningful question is thus how large a possible age spread, compared to the dynamical timescale of a star forming region or the crossing time of a cluster. In large star forming complexes (such as OB associations), which extend over several tens of parsecs, the crossing times are around (or even exceed) ≈ 10 Myr. A physical age spread of a few Myr is thus still "small" in such a situation.

Many careful studies of young clusters and star forming regions find no clear evidence or at most very moderate age spreads of just a few Myr (see, e.g., Moitinho et al. 2001; Preibisch et al. 2002; Stolte et al. 2004; Dahm & Hillenbrand 2007; Fűrész et al. 2008; Weights et al. 2009; Tobin et al. 2009; Dib et al. 2010; Da Rio et al. 2010; Jeffries et al. 2011, to give just a few examples). In most cases, the measured (upper limit to the) age spread is smaller than the crossing time. Such results are in good agreement with and support the scenario of fast star formation.

Acknowledgements I gratefully acknowledge funding by the German *Deutsche Forschungsgemeinschaft, DFG* project numbers PR 569/8-1 and PR 569/9-1. Additional support came from funds from the Munich Cluster of Excellence: "Origin and Structure of the Universe."

References

Alencar, S. H. P., Basri, G., Hartmann, L., & Calvet, N. 2005, A&A, 440, 595
André, P., Men'shchikov, A., Bontemps, S., et al. 2010, A&A, 518, L102
Armitage, P. J. 2010, Astrophysics of Planet Formation (Cambridge: Cambridge Univ. Press)
Armitage, P. J. 2011, ARA&A, 49, 195

Balbus, S. A., & Hawley, J. F. 1998, Reviews of Modern Physics, 70, 1
Ballesteros-Paredes, J., & Hartmann, L. 2007, Revista Mexicana de Astronomía y Astrofísica, 43, 123
Ballesteros-Paredes, J., Klessen, R. S., Mac Low, M.-M., & Vazquez-Semadeni, E. 2007, Protostars and Planets V, 63
Bally, J. 2008, Handbook of Star Forming Regions, Volume I, ed. B. Reipurth, ASP, 459
Banerjee, R., Vázquez-Semadeni, E., Hennebelle, P., & Klessen, R. S. 2009, MNRAS, 398, 1082
Baraffe, I., & Chabrier, G. 2010, A&A, 521, A44
Baraffe, I., Chabrier, G., Allard, F., & Hauschildt, P. H. 1998, A&A, 337, 403
Baraffe, I., Chabrier, G., Allard, F., & Hauschildt, P. H. 2002, A&A, 382, 563
Baraffe, I., Chabrier, G., & Gallardo, J. 2009, ApJ, 702, L27
Baume, G., Vázquez, R. A., Carraro, G., & Feinstein, A. 2003, A&A, 402, 549
Benz, A. O., & Güdel, M. 2010, ARA&A, 48, 241
Blaauw, A. 1964, ARA&A, 2, 213
Boulard, M.-H., Caux, E., Monin, J.-L., Nadeau, D., & Rowlands, N. 1995, A&A, 300, 276
Bouvier, J., Alencar, S. H. P., Harries, T. J., Johns-Krull, C. M., & Romanova, M. M. 2007, Protostars and Planets V, eds. B. Reipurth, D. Jewitt, & K. Keil (Tucson, AZ: University of Arizona Press), 479
Bouvier, J., Covino, E., Kovo, O., et al. 1995, A&A, 299, 89
Briceño, C., Calvet, N., Hernández, J., et al. 2005, AJ, 129, 907
Briceño, C., Preibisch, T., Sherry, W. H., et al. 2007, Protostars and Planets V, eds. B. Reipurth, D. Jewitt, & K. Keil (Tucson, AZ: University of Arizona Press), 345
Brickhouse, N. S., Cranmer, S. R., Dupree, A. K., Luna, G. J. M., & Wolk, S. 2010, ApJ, 710, 1835
Brown, A. G. A., de Geus, E. J., & de Zeeuw, P. T. 1994, A&A, 289, 101
Cannon, J. M., Walter, F., Bendo, G. J., et al. 2005, ApJ, 630, L37
Casanova, S., Montmerle, T., Feigelson, E. D., & Andre, P. 1995, ApJ, 439, 752
Chelli, A. 1999, A&A, 342, 763
Cieza, L. A., Kessler-Silacci, J. E., Jaffe, D. T., Harvey, P. M., & Evans, N. J., II 2005, ApJ, 635, 422
Connelley, M. S., & Greene, T. P. 2010, AJ, 140, 1214
Currie, T., Hernandez, J., Irwin, J., et al. 2010, ApJS, 186, 191
Da Rio, N., Gouliermis, D. A., & Gennaro, M. 2010, ApJ, 723, 166
Dahm, S. E., & Hillenbrand, L. A. 2007, AJ, 133, 2072
D'Antona, F., & Mazzitelli, I. 1994, ApJS, 90, 467
de Bruijne, J. H. J. 1999, MNRAS, 310, 585
Deharveng, L., Zavagno, A., Schuller, F., et al. 2009, A&A, 496, 177
Dib, S., Shadmehri, M., Padoan, P., et al. 2010, MNRAS, 405, 401
Dullemond, C. P., & Monnier, J. D. 2010, ARA&A, 48, 205
Duquennoy, A., & Mayor, M. 1991, A&A, 248, 485
Elmegreen, B. G. 2000, ApJ, 530, 277
Elmegreen, B. G. 2007, ApJ, 668, 1064
Ercolano, B., Clarke, C. J., & Drake, J. J. 2009, ApJ, 699, 1639
Feigelson, E. D., & Montmerle, T. 1999, ARA&A, 37, 363
Fűrész, G., Hartmann, L. W., Megeath, S. T., Szentgyorgyi, A. H., & Hamden, E. T. 2008, ApJ, 676, 1109
Flaherty, K. M., Muzerolle, J., Rieke, G., et al. 2011, ApJ, 732, 83
Gahm, G. F., Walter, F. M., Stempels, H. C., Petrov, P. P., & Herczeg, G. J. 2008, A&A, 482, L35
Garcia, P. J. V. 2011, Physical Processes in Circumstellar Disks around Young Stars (Chicago, IL: University of Chicago Press)
Garcia Lopez, R., Natta, A., Testi, L., & Habart, E. 2006, A&A, 459, 837
Getman, K. V., Feigelson, E. D., Broos, P. S., Micela, G., & Garmire, G. P. 2008, ApJ, 688, 418
Getman, K. V., Flaccomio, E., Broos, P. S., et al. 2005, ApJS, 160, 319

Gritschneder, M., Burkert, A., Naab, T., & Walch, S. 2010, ApJ, 723, 971
Gullbring, E., Calvet, N., Muzerolle, J., & Hartmann, L. 2000, ApJ, 544, 927
Hartmann, L. 2001a, Accretion Processes in Star Formation (Cambridge: Cambridge Univ. Press)
Hartmann, L. 2001b, AJ, 121, 1030
Hartmann, L. 2003, ApJ, 585, 398
Hartmann, L., Ballesteros-Paredes, J., & Bergin, E. A. 2001, ApJ, 562, 852
Hartmann, L., & Kenyon, S. J. 1996, ARA&A, 34, 207
Heitsch, F., Hartmann, L. W., & Burkert, A. 2008, ApJ, 683, 786
Hennebelle, P., Banerjee, R., Vázquez-Semadeni, E., Klessen, R. S., & Audit, E. 2008, A&A, 486, L43
Hennekemper, E., Gouliermis, D. A., Henning, T., Brandner, W., & Dolphin, A. E. 2008, ApJ, 672, 914
Herbig, G. H. 1946, PASP, 58, 163
Herbig, G. H. 1950, ApJ, 111, 15
Herbig, G. H. 1954, ApJ, 119, 483
Herbig, G. H. 1957, in Non-stable Stars, IAU Symp. 3, ed. G. H. Herbig, 3
Herbig, G. H. 1960, ApJS, 4, 337
Herbig, G. H. 1998, ApJ, 497, 736
Hillenbrand, L. A. 1997, AJ, 113, 1733
Hillenbrand, L. A., Bauermeister, A., & White, R. J. 2008, in 14th Cambridge Workshop on Cool Stars, Stellar Systems, and the Sun, Astronomical Society of the Pacific Conference Series, 384, ed. G. van Belle, 200 (arXiv: astro-ph/0703642)
Hillenbrand, L. A., & White, R. J. 2004, ApJ, 604, 741
Hind, J. R. 1864, MNRAS, 24, 65
Huff, E. M., & Stahler, S. W. 2007, ApJ, 666, 281
Jeffries, R. D., Littlefair, S. P., Naylor, T., & Mayne, N. J. 2011, MNRAS, 1538
Joy, A. H. 1945, ApJ, 102, 168
Joy, A. H. 1949, ApJ, 110, 424
Kraus, S., Hofmann, K.-H., Benisty, M., et al. 2008a, A&A, 489, 1157
Kraus, S., Hofmann, K.-H., Preibisch, T., & Weigelt, G. 2010, in Revista Mexicana de Astronomia y Astrofisica Conference Series 38, 63
Kraus, S., Preibisch, T., & Ohnaka, K. 2008b, ApJ, 676, 490
Kretzschmar, M., de Wit, T. D., Schmutz, W., et al. 2010, Nature Physics, 6, 690
Krivov, A. V. 2010, RAA (Research in Astronomy and Astrophysics), 10, 383
Kroupa, P. 2002, Science, 295, 82
Leone, F. 2007, ApJ, 667, L175
Littlefair, S. P., Naylor, T., Burningham, B., & Jeffries, R. D. 2005, MNRAS, 358, 341
Littlefair, S. P., Naylor, T., Mayne, N. J., Saunders, E., & Jeffries, R. D. 2011, MNRAS, 413, L56
Luhman, K. L. 1999, ApJ, 525, 466
Luhman, K. L., Lada, E. A., Muench, A. A., & Elston, R. J. 2005, ApJ, 618, 810
Luhman, K. L., Rieke, G. H., Lada, C. J., & Lada, E. A. 1998, ApJ, 508, 347
Martín, E. L. 1998, AJ, 115, 351
Mathis, J. S. 1990, ARA&A, 28, 37
Men'shchikov, A. B., & Henning, T. 1997, A&A, 318, 879
Meyer, M. R., Calvet, N., & Hillenbrand, L. A. 1997, AJ, 114, 288
Moitinho, A., Alves, J., Huélamo, N., & Lada, C. J. 2001, ApJ, 563, L73
Molinari, S., Swinyard, B., Bally, J., et al. 2010, A&A, 518, L100
Morales-Calderón, M., Stauffer, J. R., Hillenbrand, L. A., et al. 2011, ApJ, 733, 50
Muzerolle, J., D'Alessio, P., Calvet, N., & Hartmann, L. 2004, ApJ, 617, 406
Muzerolle, J., Flaherty, K., Balog, Z., et al. 2009, ApJ, 704, L15

Oey, M. S., Watson, A. M., Kern, K., & Walth, G. L. 2005, AJ, 129, 393
Orlando, S., Reale, F., Peres, G., & Mignone, A. 2011, MNRAS, 415, 3380
Palla, F., Randich, S., Pavlenko, Y. V., Flaccomio, E., & Pallavicini, R. 2007, ApJ, 659, L41
Palla, F., & Stahler, S. W. 1999, ApJ, 525, 772
Palla, F., & Stahler, S. W. 2000, ApJ, 540, 255
Pflamm-Altenburg, J., & Kroupa, P. 2007, MNRAS, 375, 855
Povich, M. S., Townsley, L. K., Broos, P. S., et al. 2011, ApJS, 194, 6
Preibisch, T., Brown, A. G. A., Bridges, T., Guenther, E., & Zinnecker, H. 2002, AJ, 124, 404
Preibisch, T., & Feigelson, E. D. 2005, ApJS, 160, 390
Preibisch, T., Hodgkin, S., Irwin, M., et al. 2011a, ApJS, 194, 10
Preibisch, T., Kim, Y.-C., Favata, F., et al. 2005, ApJS, 160, 401
Preibisch, T., Ratzka, T., Gehring, T., et al. 2011b, A&A, 530, A40
Preibisch, T., Ratzka, T., Kuderna, B., et al. 2011c, A&A, 530, A34
Preibisch, T., & Zinnecker, H. 2007, in IAU Symp. 237, eds. B. G. Elmegreen & J. Palous, 270
Preibisch, T., Zinnecker, H., & Herbig, G. H. 1996, A&A, 310, 456
Preibisch, T., & Mamajek, E. 2008, Handbook of Star Forming Regions, Volume II, ed. B. Reipurth, ASP, 235
Raghavan, D., McAlister, H. A., Henry, T. J., et al. 2010, ApJS, 190, 1
Reach, W. T., Rho, J., Young, E., et al. 2004, ApJS, 154, 385
Reipurth, B., Jewitt, D., & Keil, K. 2007, Protostars and Planets V (Tucson, AZ: University of Arizona Press)
Rieke, G. H. 2009, Experimental Astronomy, 25, 125
Robitaille, T. P., Whitney, B. A., Indebetouw, R., Wood, K., & Denzmore, P. 2006, ApJS, 167, 256
Romanova, M. M., Kulkarni, A. K., & Lovelace, R. V. E. 2008, ApJ, 673, L171
Sacco, G. G., Randich, S., Franciosini, E., Pallavicini, R., & Palla, F. 2007, A&A, 462, L23
Schmidt, T., Guenther, E., Hatzes, A. P., et al. 2005, Astronomische Nachrichten, 326, 667
Sestito, P., Palla, F., & Randich, S. 2008, A&A, 487, 965
Siess, L., Dufour, E., & Forestini, M. 2000, A&A, 358, 593
Siess, L., Forestini, M., & Bertout, C. 1999, A&A, 342, 480
Slesnick, C. L., Hillenbrand, L. A., & Carpenter, J. M. 2008, ApJ, 688, 377
Smith, N., & Brooks, K. J. 2008, in Handbook of Low Mass Star Forming Regions, Volume II: The Southern Sky, ASP Monograph Publications, 5, ed. Bo Reipurth, 138
Soderblom, D. R. 2010, ARA&A, 48, 581
Solomon, P. M., Sanders, D. B., & Scoville, N. Z. 1979, in IAU Symp. 84, The Large-Scale Characteristics of the Galaxy, ed. W. B. Burton, 35
Stahler, S. W., & Palla, F. 2005, The Formation of Stars (Weinheim: Wiley-VCH)
Stapelfeldt, K. R., Krist, J. E., Menard, F., et al. 1998, ApJ, 502, L65
Stassun, K. G., Hebb, L., López-Morales, M., & Prša, A. 2009, in IAU Symp. 258, eds. E. E. Mamajek, D. R. Soderblom, & R. F. G. Wyse, 161
Stassun, K. G., van den Berg, M., Feigelson, E., & Flaccomio, E. 2006, ApJ, 649, 914
Stolte, A., Brandner, W., Brandl, B., Zinnecker, H., & Grebel, E. K. 2004, AJ, 128, 765
Strassmeier, K. G. 2006, Ap&SS, 304, 333
Strom, S. E., Strom, K. M., Yost, J., Carrasco, L., & Grasdalen, G. 1972, ApJ, 173, 353
Tan, J. C., Krumholz, M. R., & McKee, C. F. 2006, ApJ, 641, L121
Tobin, J. J., Hartmann, L., Furesz, G., Mateo, M., & Megeath, S. T. 2009, ApJ, 697, 1103
Tognelli, E., Prada Moroni, P. G., & Degl'Innocenti, S. 2011, A&A, 533, A109
Tout, C. A., Livio, M., & Bonnell, I. A. 1999, MNRAS, 310, 360
van Boekel, R., Min, M., Leinert, C., et al. 2004, Nature, 432, 479
Vorobyov, E. I., & Basu, S. 2006, ApJ, 650, 956
Walter, F. M., Vrba, F. J., Mathieu, R. D., Brown, A., & Myers, P. C. 1994, AJ, 107, 692

Ward-Thompson, D., & Whitworth, A. P. 2011, An Introduction to Star Formation (Cambridge: Cambridge Univ. Press)
Weights, D. J., Lucas, P. W., Roche, P. F., Pinfield, D. J., & Riddick, F. 2009, MNRAS, 392, 817
Whitney, B. A., Wood, K., Bjorkman, J. E., & Cohen, M. 2003, ApJ, 598, 1079
Wilking, B. A., Schwartz, R. D., & Blackwell, J. H. 1987, AJ, 94, 106
Williams, J. P., & Cieza, L. A. 2011, ARA&A, 49, 67
Withbroe, G. L. 2009, Sol. Phys., 257, 71
Wolf, S., Padgett, D. L., & Stapelfeldt, K. R. 2003, ApJ, 588, 373
Wolk, S. J., Harnden, F. R., Jr., Flaccomio, E., et al. 2005, ApJS, 160, 423
Wuchterl, G., & Tscharnuter, W. M. 2003, A&A, 398, 1081
Zavagno, A., Anderson, L. D., Russeil, D., et al. 2010, A&A, 518, L101
Zinnecker, H., Krabbe, A., McCaughrean, M. J., et al. 1999, A&A, 352, L73
Zinnecker, H., & Mathieu, R. (eds.) 2001, IAU Symp. 200, The Formation of Binary Stars
Zinnecker, H., & Yorke, H. W. 2007, ARA&A, 45, 481